CHALMERS
UNIVERSITY OF TECHNOLOGY

A two-step parameter extraction methodology for graphene field-effect transistors

Paper presented at ICMTS 2022

A two-step parameter extraction methodology for graphene field-effect transistors

Kjell Jeppson, *Life Senior Member, IEEE*
Chalmers University of Technology
Gothenburg, Sweden

***Abstract* — Accurate device models and parameter extraction methods are of utmost importance for characterizing graphene field-effect transistors and for predicting their performance in circuit applications. For DC characterization, accurate extraction of the transconductance parameter (i.e., low-field mobility) and series resistance is of particular importance. In this paper, methods for extraction of these parameters will be discussed.**

A first-order mobility degradation model that can be used to separate information about mobility degradation and series resistance for a set of graphene field-effect transistors will also be discussed.

Keywords—graphene field-effect transistors, model parameter extraction, charge-carrier mobility, series resistance, mobility.

I. Introduction

Admittedly, it might appear somewhat late to come with advice on how to extract graphene field-effect transistor (GFET) model parameters from current-voltage measurements now more than ten years after the most widely used models were published. Nevertheless, consistent parameter extraction procedures are important, particularly when far-reaching conclusions tend to be drawn based on the extracted parameter values concerning charge-carrier mobility on the one hand, and series and contact resistances on the other hand. Before discussing the parameter extraction process, the model used to describe the GFET transfer characteristic is reviewed. Thereafter, important extraction procedures are applied to three kinds of GFETs, i) ideal GFETs described by synthetic data generated from the model, ii) top-gated GFETs based on exfoliated graphene, and iii) top-gated GFETs based on chemical vapor deposited (CVD) graphene.

II. GFET Modeling

Graphene field-effect transistors are usually characterized for series resistance and low-field mobility using the resistance model proposed by Meric et al. [1] and adapted by Kim et al. [2]. This model is basically a four parameter model (k, R_{eff}, V_{Dirac}, and V_0) that can be written

$$R_{DS} = R_{eff} + \left(k\sqrt{V_{GSO}^2 + V_0^2} \right)^{-1}, \tag{1}$$

where k is the transconductance parameter, R_{eff} the effective series resistance including the sum of the contact and access resistances (R_C), and the excess resistance caused by mobility degradation due to the transversal field, V_{GSO} the gate overdrive voltage wrt to the minimum conductance point (V_{Dirac}),

$$V_{GSO} = V_{GS} - V_{Dirac} - V_{DS}/2, \tag{2}$$

and V_0 is the residual gate voltage due to the existence of residual charges [3]. As usual, V_{GS} and V_{DS} are the gate to source and drain to source voltages, respectively. The resistance model in (1) is based on a transversal field model

$$E_t = \sqrt{V_{GSO}^2 + V_0^2}\,/\,t_{ox}, \tag{3}$$

where t_{ox} is the thickness of the gate dielectric, and a lateral field

$$E_{int} = \left(V_{DS} - R_C I_D\right)/L, \tag{4}$$

where I_D is the drain current, R_C the series resistance, and L the gate length. Assuming a first-order mobility degradation model due to the transversal field as proposed in [4],

$$\mu = \frac{\mu_0}{1 + \theta\sqrt{V_{GSO}^2 + V_0^2}}, \tag{5}$$

where μ_0 is the low-field mobility, and θ the mobility degradation coefficient, the following current model is obtained

$$I_D = \frac{kV_{DS}\sqrt{V_{GSO}^2 + V_0^2}}{1 + kR_{eff}\sqrt{V_{GSO}^2 + V_0^2}}. \tag{6}$$

This work was supported in part by the third core project of the Graphene Flagship; a project financed by the European Union.
Email: kjell.jeppson@chalmers.se
http://orcid.org/0000-0001-5049-9303

Here $k=(W/L)k'$ with $k'=\mu_0 C_{ox}$ being the GFET process transconductance parameter, W the channel width, and $C_{ox}=\varepsilon_{ox}/t_{ox}$ the capacitance per unit area of the gate dielectric (permittivity ε_{ox}). The effective resistance $R_{eff}=R_C+\theta/k$ is the sum of the series resistance R_C and the contribution θ/k to the channel resistance caused by mobility degradation. So even if mobility degradation was not part of the original description of the model, a model sometimes referred to as a "constant-mobility model", such information can in fact be found embedded in the effective "series" resistance. As an aside, it might be interesting to note that circuit designers already in the 1960's added a series resistance to the MOSFET equivalent circuit to model the field-induced mobility degradation in the channel [5]. The modified GFET resistance model now becomes

$$R_{DS} = R_C + \underbrace{\frac{L}{Wk'}\left(\theta + \frac{1}{\sqrt{V_{GSO}^2 + V_0^2}}\right)}_{\text{channel resistance } \sim L}. \qquad (7)$$

The observation of a series resistance R_C independent of the channel length, and a channel resistance proportional to the channel length, makes it possible to separate the two contributions to the effective resistance R_{eff} from the slope and y-intercept of an R_{eff} vs. L plot.

III. Parameter Extraction

In the previous section, some background information about the model used to describe the GFET transfer characteristics was presented. In this section, an extraction methodology for obtaining the four GFET model parameters, k, R_{eff}, V_{Dirac} and V_0, from experimental data will be discussed. Data from three types of GFETs will be used to illustrate problems encountered during the parameter extraction process, i) ideal GFETs described by synthetic data generated from the model, ii) top-gated GFETs based on exfoliated graphene, and iii) top-gated GFETs based on CVD graphene.

The use of synthetic data for extracting the GFET model parameters will provide a good start for reviewing the proposed extraction process since such devices are ideal and their model parameters already known.

Compared to the extraction of the corresponding MOSFET parameters, k, R_{eff}, and threshold voltage V_T, the fourth GFET model parameter V_0 causes some additional problems. On the other hand the Dirac voltage is well defined and easy to extract from the minimum conduction point. The threshold voltage of a MOSFET is not equally well defined.

For MOSFETs, the three-point extraction process is a quick and simple process for extracting the three MOSFET model parameters from three representative experimental data points by solving a system of three linear equations [6][7]. Usually two data points are chosen well into the linear region ($V_{GS}>>V_T$) and one data point close to the threshold voltage.

This direct extraction process was applied to synthetic GFET data generated by the model using k=25 mA/V^2, R_{eff}=40 Ω, V_{Dirac}=0, and five different residual voltages (0.1, 0.3, 0.5, 0.7, and 1.0 V). The five GFET synthetic transfer curves (I_D vs. V_{GS}) are shown in Fig. 1 (symbols). First, the three data points used for parameter extraction were those obtained for gate

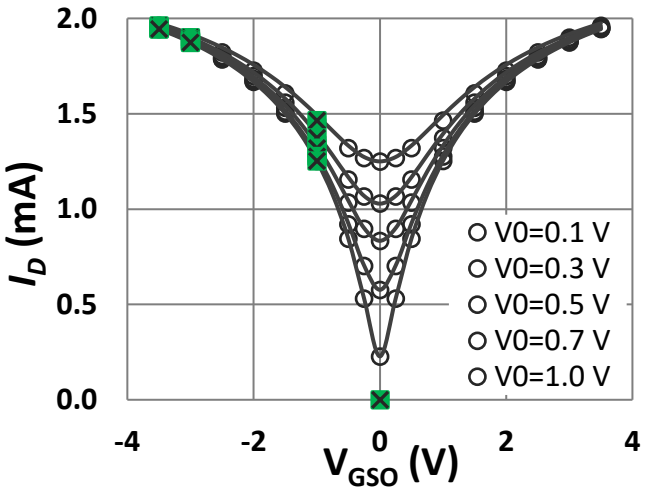

Fig. 1. Synthetic I_D versus gate-source voltage data for five different residual voltages (symbols), and the corresponding models using model parameters obtained by using the 3-point extraction method.

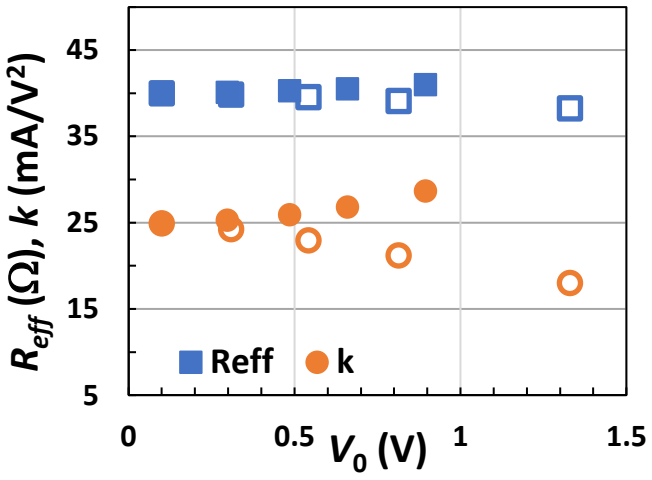

Fig. 2. Effective resistances and transconductance parameters extracted for the five residual voltages using data from gate voltages −3.5, −3, −1 V (open symbols) and from −3.5, −3, 0 V (filled symbols).

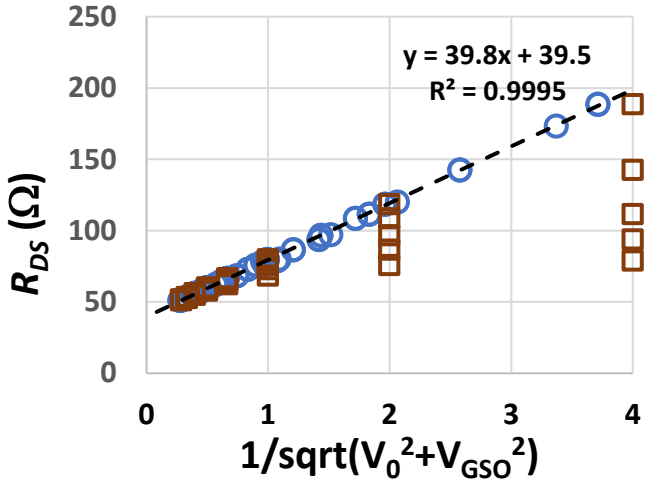

Fig. 3. Synthetic R_{DS} data vs. $1/\sqrt{(V_0^2+V_{GSO}^2)}$ with trendline yielding k=25.13 A/V^2 and effective resistance 39.5 Ω (circles). Also shown is the same resistance plotted vs. $1/V_{GSO}$ assuming V_0=0 (squares).

voltages –3.5, –3, and –1 V (cross symbols in Fig. 1). The values extracted for parameters k, R_{eff}, and V_0, are shown in Fig. 2 (open symbols). As shown, the resistance is accurately extracted to within a few per cent, while the values for k and V_0 are a somewhat off their nominal values. Furthermore, the method did not always return the correct Dirac voltage.

For improving the model parameter extraction the third data point was moved from V_{GS} = –1 to V_{GS} =0 V with current set to zero. The extracted parameter values are shown in Fig. 2 (closed symbols). The residual voltage was calculated by fitting the model the minimum current at the Dirac point. The errors in extracted values for parameters k and R_{eff} were reduced to half; the extracted resistance being within 1 Ω (2.5 %) and the transconductance parameter within 15%. The models shown in Fig. 1 (solid lines) obtained using these model parameter values show good agreement with the synthetic data.

The second choice of experimental data for the extraction i.e., assuming a known Dirac voltage and a negligible residual voltage (V_0=0), is identical to selecting two resistance values in the $1/V_{GSO}$ plane and using the slope and y-intercept of the trendline to separate k from R_{eff}. This is a well-known method presented by de La Moneda et al. already in 1982 even if they of course used more than two data points [8]. The disadvantage of their method when it comes to MOSFETs is that the threshold voltage has to be determined separately from the other two parameters (k and R_{eff}), while in a method like the three-point method all three parameters are extracted together. However, for GFETs this is not a problem since the Dirac voltage is well defined by the minimum conduction point. For this reason, the method proposed by de La Moneda et al. appears to be an appropriate method for separating GFET low-field properties (k) from the effects of mobility degradation and series resistance (R_{eff}). Since the extracted model parameters (k, R_{eff}) generates a value for the residual voltage, an iterative process can be applied, at least for ideal GFET devices, to successively obtain improved model parameters from the trendline of an R_{DS} vs. $1/\sqrt{(V_0^2 + V_{GSO}^2)}$ graph. Such graphs are shown in Fig. 3 where the synthetic data points, initially showing a nonlinear behavior vs. $1/V_{GSO}$ (V_0=0, squares), line up almost perfectly vs. $1/\sqrt{(V_0^2 + V_{GSO}^2)}$ once appropriate values for V_0 are found (circles).

In conclusion, the suggested two-step extraction method based on an initial procedure using the 3-point method for obtaining preliminary model parameter values followed by a second step validating the extracted model parameters using R_{DS} vs. $1/\sqrt{(V_0^2 + V_{GSO}^2)}$ plots was shown to accurately return the parameters used to generate the synthetic data. In the next two subsections, the proposed extraction process will be applied to top-gated GFETs fabricated both on exfoliated graphene and on CVD graphene.

A. Top-gated GFETs on exfoliated graphene

In this subsection, the device under test is a 2×10 µm wide, 1 µm long, top-gated GFET fabricated on exfoliated graphene, the measured transfer characteristic of which is shown in Fig. 4 [3]. The immediately obvious difference between this device and the synthetic devices discussed above is that it is not symmetrical about the Dirac point. This can be explained by the different contact resistances for holes and electrons. However, parameter extraction can still be performed the same way as

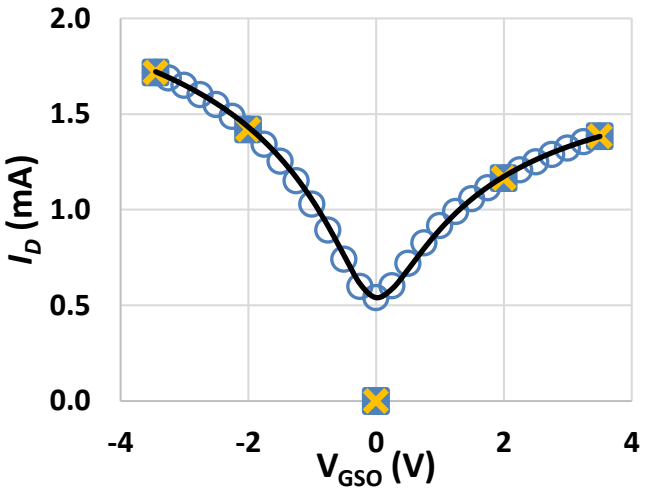

Fig. 4. Graph showing an experimental transfer characteristic of a top-gated GFET on exfoliated graphene (symbols) and the model (solid line) with model parameters obtained from the three cross-marked data points for the hole and electron sides, respectively. Experimental data from [3].

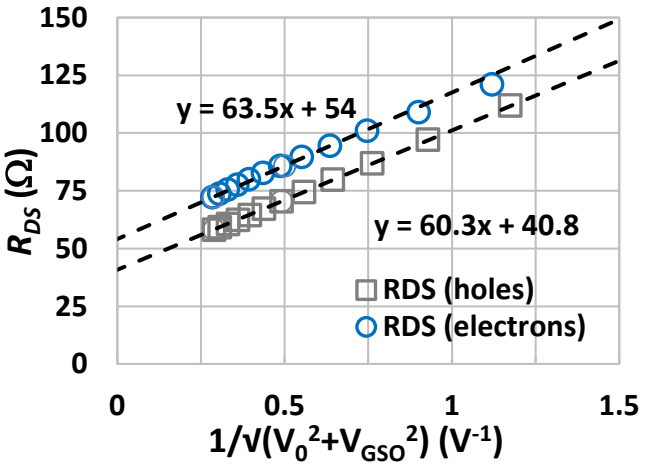

Fig. 5. Graph showing experimental R_{DS} vs. $1/\sqrt{(V_0^2+V_{GSO}^2)}$ for a top-gated GFET on exfoliated graphene.

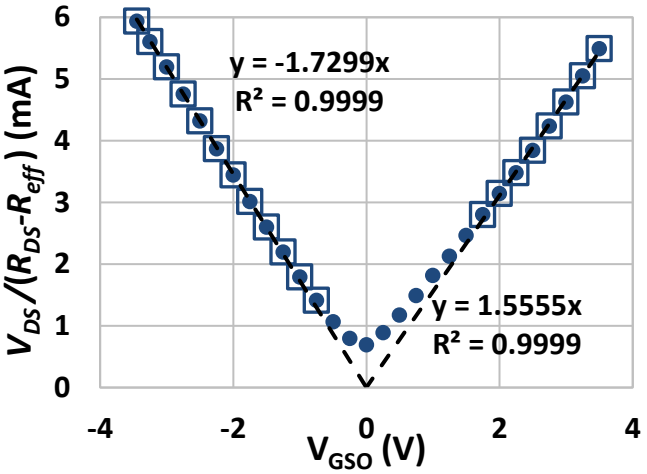

Fig. 6. Graph showing $I_D=V_{DS}/(R_{DS}-R_S)$ vs. V_{GSO} for a top-gated GFET on exfoliated graphene.

previously described if performed separately for holes and electrons. This is also shown in Fig. 4 where the model was fitted to experimental data using the model parameters obtained using the three data points indicated by cross symbols. The behavior of this top-gated GFET on exfoliated graphene is very close to ideal, particularly for holes being the charge carriers. This was confirmed by the linearity of the R_{DS} vs. $1/\sqrt{(V_0^2 + V_{GSO}^2)}$ graphs in Fig. 5. The extracted effective resistances are 41 Ω and 54 Ω for V_{GSO}<0 and V_{GSO}>0, respectively. As indicated by the almost parallel trendlines, the hole and electron low-field mobilities are almost identical. One way to validate the extracted model parameter values is to replot the transfer characteristic with the effective resistance subtracted. This is shown in Fig. 6, where the trendlines return the same values for model parameter k as the values derived from the trendline slopes in Fig. 5.

B. Top-gated GFETs on CVD graphene

Finally, let us apply the parameter extraction process to top-gated GFETs on chemical vapor deposition (CVD) graphene. These devices are more complicated to model because of the inhomogenouos properties of CVD graphene. This becomes immediately obvious when comparing the performance of the individual fingers of a dual-channel GFET. Not only can the Dirac point differ between the two channels, but also the other model parameters can vary between channels and probably also along channels.

Fig. 7 shows the experimentally obtained resistance curves of two top-gated GFETs on CVD graphene published in [9]. As described in [9], both devices were fabricated on CVD graphene transferred to SiO_2/Si substrates, the only difference being one of the devices having an Al_2O_3 interfacial layer for increasing the charge-carrier saturation velocity due to the higher optical phonon energy of Al_2O_3 compared to that of SiO_2. Fig. 8 shows the experimental data for the same two devices replotted as drain current versus the gate overdrive voltage V_{GSO} together with the models obtained by using the extraction process described above. The main difference between devices concerns the effective resistances being 19 Ω and 11 Ω for the devices with and without the Al_2O_3 interfacial layer, respectively. However, the transconductance parameters are almost the same for both devices, which is illustrated by Fig. 9 showing the transfer characteristics replotted with the effective resistances subtracted. When comparing the top-gated GFETs on CVD graphene with the one on exfoliated graphene from the previous subsection, the different channel geometries must be taken into account. While the process transconductance parameter for the GFET on exfoliated graphene is k'=0.83 mA/V^2, it is about 0.67 mA/V^2 for the two GFETs on CVD graphene.

So far, some examples of successful parameter extraction resulting in good model fit to experimental data have been given. However, not all GFET devices on CVD graphene are that easy to characterize, but rather leave you in doubt on how to best perform the parameter extraction. One such example is shown in Fig. 10 for a top-gated GFET on CVD graphene transferred to a diamond substrate [10]. Here, a model has been fitted to the experimentally obtained resistance curve using model parameters from [10]. While the model fit shown in Fig. 10 appears acceptable to the eye, a replot of the current model,

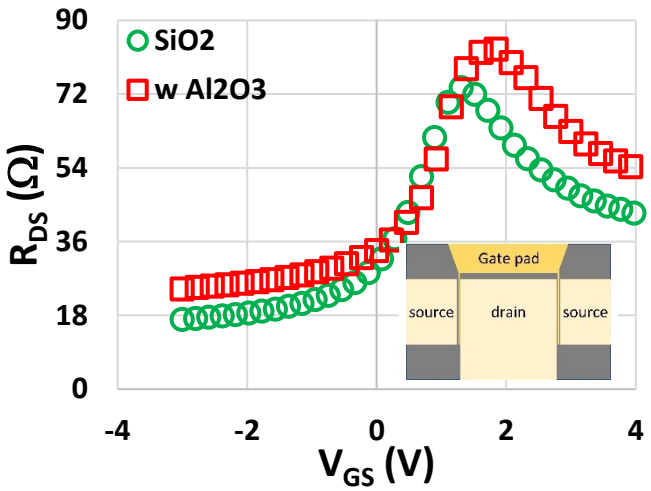

Fig. 7. Graph showing experimental transfer characteristics of two top-gated GFETs on CVD graphene fabricated with and without the Al_2O_3 interfacial layer used to increase charge-carrier saturation velocity. Inset shows schematic representation of the GFET layout. Experimental data from [9].

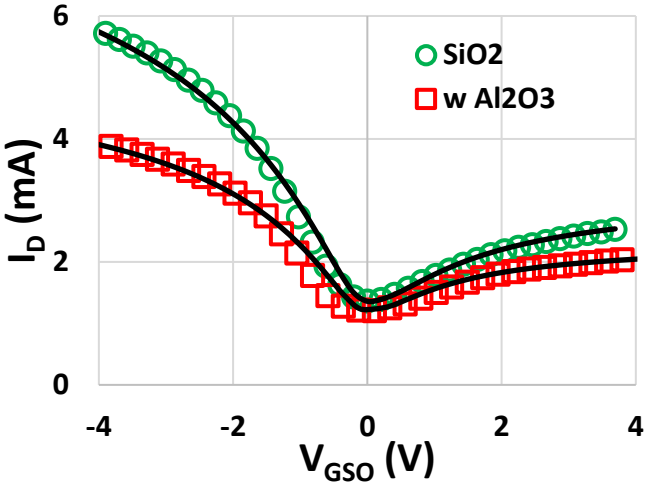

Fig. 8. Graph showing models fitted to the same experimental data as in Fig. 7 replotted as drain current vs. gate overdrive voltage.

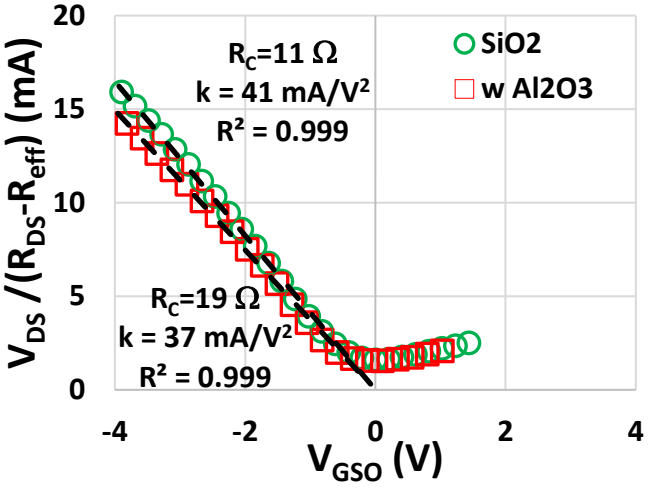

Fig. 9. Graph showing $I_D=V_{DS}/(R_{DS}-R_{eff})$ vs. gate overdrive voltage validating almost identical transconductance parameters.

using the same model parameters, fitted to drain current data instead of using resistance data, reveals how the extraction process appears to have failed capturing the transconductance

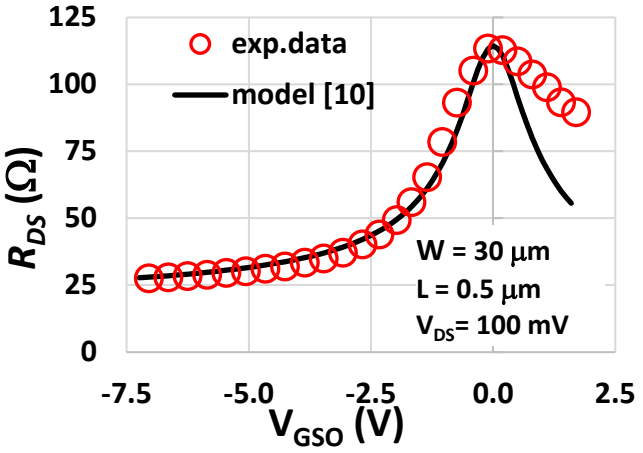

Fig. 10. Model fitted to experimental $R_{DS}=V_{DS}/I_D$ data for a top-gated GFET on diamond substrate [10].

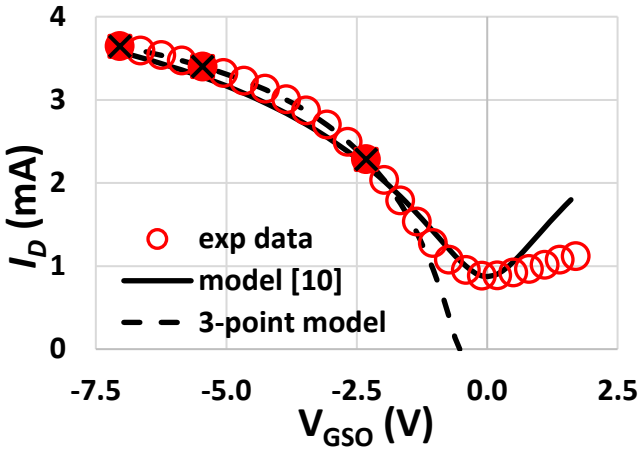

Fig. 11. Model (solid line) using the same parameters as in Fig. 10 fitted to drain current data (symbols). Also shown is the model obtained using parameters extracted from the three high-lighted data points (dashed line).

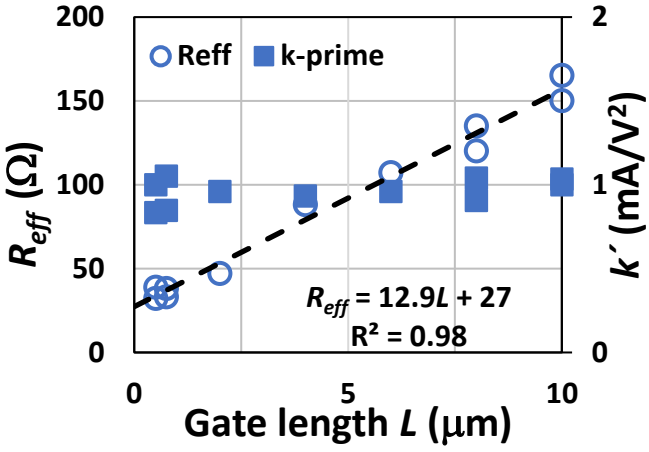

Fig. 12. Effective resistance and process transconductance parameter vs. gate length for a set of top-gated GFETs on exfoliated graphene.

parameter (read low-field mobility). Fig. 11 also shows an alternative model obtained by direct extraction using three data point. The use of these alternative model parameters, returns a model showing excellent field-effect behavior of the GFET device. However, this model does not capture the correct Dirac voltage. There is a considerable difference between the trans-conductance parameters obtained by the two methods, 25.8 vs. 15.8 mA/V^2.

The need for extracting correct values for parameters k and R_{eff} is important not only for extracting the low-field mobility from parameter k, but also for separating the two effects contributing to the effective resistance i.e., the series resistance between the GFET and its external pads, and the mobility degradation due to the transversal field as modeled by equation (5). One such attempt is shown in Fig. 12 where the effective resistance R_{eff} has been plotted as a function of the gate length for a set of 15 µm wide GFETs on CVD graphene with the same process transconductance parameter (read low-field mobility). This graph indicates a series resistance of 27 Ω and a mobility degradation coefficient θ of 0.19 V^{-1} for this set of devices.

IV. Conclusions

In conclusion, a two-step GFET parameter extraction process has been proposed and evaluated for robustness and reliability. The 3-point direct extraction method was shown to be a simple tool for rapid extraction of the model parameters by solving a system of linear equations provided that data points are properly selected. For improved accuracy, the trendline of an R_{DS} vs. $1/V_{GSO}$ graph efficiently separates the effective resistance from the transconductance parameter. A plot of the drain current with the influence of the effective resistance subtracted i.e., a plot of $V_{DS}/(R_{DS}-R_{eff})$ vs. V_{GS}, should return a linear dependence on V_{GS} for $V_{GSO}>>V_0$ with the same transconductance parameter. This also validates that a first-order dependence of the low-field mobility on the transversal field can be derived from the effective resistance.

Acknowledgement

The author would like to thank Dr. Muhammad Asad and professor Jan Stake for their support of this work. Dr. Asad is also acknowledged for fabricating and characterizing the top-gated GFETs on CVD graphene as part of his Ph. D. thesis.

References

[1] Meric, I., Han, M., Young, A. et al. "Current saturation in zero-bandgap, top-gated graphene field-effect transistors." *Nature Nanotech* 3, 654–659 (2008). https://doi.org/10.1038/nnano.2008.268

[2] S. Kim, J. Nah, I. Jo, D. Shahrjerdi, L. Colombo, Z. Yao, E. Tutuc, and S. K. Banerjee, "Realization of a high mobility dual-gated graphene field-effect transistor with Al2O3 dielectric", *Appl. Phys. Lett.*, 94, 062107, 2009. doi: 10.1063/1.3077021

[3] O. Habibpour, J. Vukusic and J. Stake, "A large-signal graphene FET model," in *IEEE Transactions on Electron Devices*, vol. 59, no. 4, pp. 968-975, April 2012. doi: 10.1109/TED.2012.2182675

[4] K. Jeppson, M. Asad and J. Stake, "Mobility Degradation and Series Resistance in Graphene Field-Effect Transistors," in *IEEE Transactions on Electron Devices*, vol. 68, no. 6, pp. 3091-3095, June 2021. doi: 10.1109/TED.2021.3074479

[5] R.H. Crawford, *MOSFET in Circuit Design*, p. 68, McGraw-Hill Book Company (June 1967) ISBN-10: 0070134758.

[6] M. F. Hamer, "First-order parameter extraction on enhancement silicon MOS transistors," *Proc. Inst. Elect. Eng.*, vol. 133, no. 2, pp. 49–54, 1986.

[7] K. O. Jeppson, "Three- and four-point Hamer-type MOSFET parameter extraction methods revisited," 2013 *IEEE International Conference on Microelectronic Test Structures (ICMTS),* 2013, pp. 141-145. doi: 10.1109/ICMTS.2013.6528161

[8] F. H. De La Moneda, H. N. Kotecha and M. Shatzkes, "Measurement of MOSFET constants," in *IEEE Electron Device Letters*, vol. 3, no. 1, pp. 10-12, Jan. 1982. doi: 10.1109/EDL.1982.25456

[9] M. Asad, K. O. Jeppson, A. Vorobiev, M. Bonmann and J. Stake, "Enhanced High-Frequency Performance of Top-Gated Graphene FETs Due to Substrate-Induced Improvements in Charge Carrier Saturation Velocity," *in IEEE Transactions on Electron Devices*, vol. 68, no. 2, pp. 899-902, Feb. 2021. doi: 10.1109/TED.2020.3046172

[10] M. Asad, "Impact of adjacent dielectrics on the high-frequency performance of graphene field-effect transistors", Ph. D. thesis, Chalmers University of Technology, Gothenburg, Sweden, Report MC2-423, ISSN 1652-0769 (2021)